

Characteristics Investigation of Organic Light Emitting Diodes Using Numerical Device Simulation

Yong Soo Lee, Jae-Hoon Park and Jong Sun Choi
Electrical Engineering Materials & Devices Lab.

Dept. of Electrical, Information & Control Eng., Hongik University, Seoul, 121-791, Korea
Phone : +82-2-320-1488 , E-mail : gyslee0@wow1.hongik.ac.kr

Abstract

We have investigated the electrical characteristics of the organic light emitting diodes (OLEDs) using the numerical device simulation. The current-voltage characteristics, the charge carrier concentrations, and the recombination rate profiles are presented. The simulation results of the effects of the various device parameters on the device characteristics are discussed.

1. Introduction

The organic light emitting diodes (OLEDs) based on the small molecules or conjugated polymers have been paid much attention due to their possible applications for flat panel displays. A lot of investigations for the commercial applications have been pursued, but some of the important electrical characteristics have not been revealed yet.

Although the OLEDs have been under intensive study in the last decade, there is much room both for further understanding of the fundamental device physics and for improvement of device technologies. At this stage of development, the device simulation becomes very helpful in that it would help to explain the various experimental results and also to get insight of the device physics [1-6, 11].

In this study, we have performed the numerical device simulation of the double layer OLEDs. The drift-diffusion current transport, the field-dependent carrier mobility, the exponential trap distribution, and the Langevin recombination models are included in this computer model. The current-voltage characteristics and the spatial distribution of the charge carrier concentrations and the recombination rate profile in the device structure will be presented.

2. Models

The device model in this study has been described in elsewhere [6]. The computer model for the OLEDs is based on the solution to the Poisson's and

continuity equations for hole and electron, and the

hole and electron currents are given by the drift-diffusion transport equation. The charge carrier mobilities are expected to be field-dependent in amorphous organic materials for OLEDs and modeled as the following equation:

$$\mu = \mu_0 \exp \sqrt{\frac{E}{E_0}} \quad (1)$$

where μ_0 and E_0 are the organic material parameters and E the electric field [7].

The double layer OLEDs has an internal interface at the organic-organic interface. The thermionic emission current and the backflowing interface recombination current were used to model the internal interface. In order to model the anode-organic layer contact, the following equations were used.

$$J_p = qv_p(p - p_{eq}) \quad (2)$$

$$J_n = -qv_n(n - n_{eq}) \quad (3)$$

where v_p and v_n are the effective surface recombination velocities for the hole and electron, respectively, and p_{eq} and n_{eq} the hole and electron concentration at the thermal equilibrium, respectively.

When the charge carriers pass over the contact barrier, they are assumed that the charge carrier concentrations are exponentially reduced.

$$J_p = q\mu_p E p \exp\left(-\frac{q\phi_h}{kT}\right) \quad (4)$$

$$J_n = q\mu_n E n \exp\left(-\frac{q\phi_e}{kT}\right) \quad (5)$$

The $\phi_{h(e)}$ is the field-dependent barrier height, and given by the following formula.

$$\phi_{h(e)} = \phi_{0h(e)} - \sqrt{\frac{qE}{4\pi\epsilon_0\epsilon_r}} \quad (6)$$

where μ_p and μ_n are the field-dependent hole and electron mobility, E the electric field, and p and n the hole and electron concentrations, respectively. Ohmic boundary condition was assumed at the cathode-organic layer contact.

The distribution of the band tail states was assumed to have an exponential energy dependence. The valence band tail and the conduction band tail were assumed to be donor-like and acceptor-like, respectively. The recombination rate was modeled by the Langevin recombination theory. If the holes and electrons are statistically independent of each other, the carrier recombination is a random process and is kinetically bimolecular.

The highly non-linear nature of the transport equations to be solved suggested the use of approximate numerical methods. The well-known finite-difference method was chosen for simplicity and accuracy. Since the dependent variables in the above models are of greatly different orders of magnitude and show a strongly different behavior in regions with the space charge, the first step towards a structural analysis of the above equations has to be appropriate normalization. The discretized equations were normalized by A. de Mari scheme [8]. For the discretization at the organic-organic internal interface nodes, the Sutherland algorithm was used [9]. The damping method was used to prevent the abrupt change by large steps when the high bias is applied.

The device simulation was performed for the conventional TPD-Alq₃ double layer structures. The important material and device parameters were optimized to have the best fit to the experimental data.

3. Results and Discussions

The simulated and measured current-voltage characteristics are shown in figure 1, where the data in a semilogarithmic scale is inserted. The thicknesses of the hole transport layer (HTL) and the electron transport layer (ETL) for the devices are 50nm, respectively. The μ_{p0} of the HTL, the other zero-field mobilities parameters and the E_0 were chosen as $1 \times 10^{-3} \text{ cm}^2/\text{Vs}$ and $1 \times 10^{-6} \text{ cm}^2/\text{Vs}$, and $2.7 \times 10^4 \text{ V/cm}$, respectively, to obtain good agreement between the simulated and the measured results.

The simulated current-voltage characteristics for different barrier height of the hole injecting contact are shown in figure 2. The increase of the current density at a given bias and the decrease of the turn on

voltage are observed with the barrier height reduction. These are consistent with the experimental results. When the anode treatment method was used, the

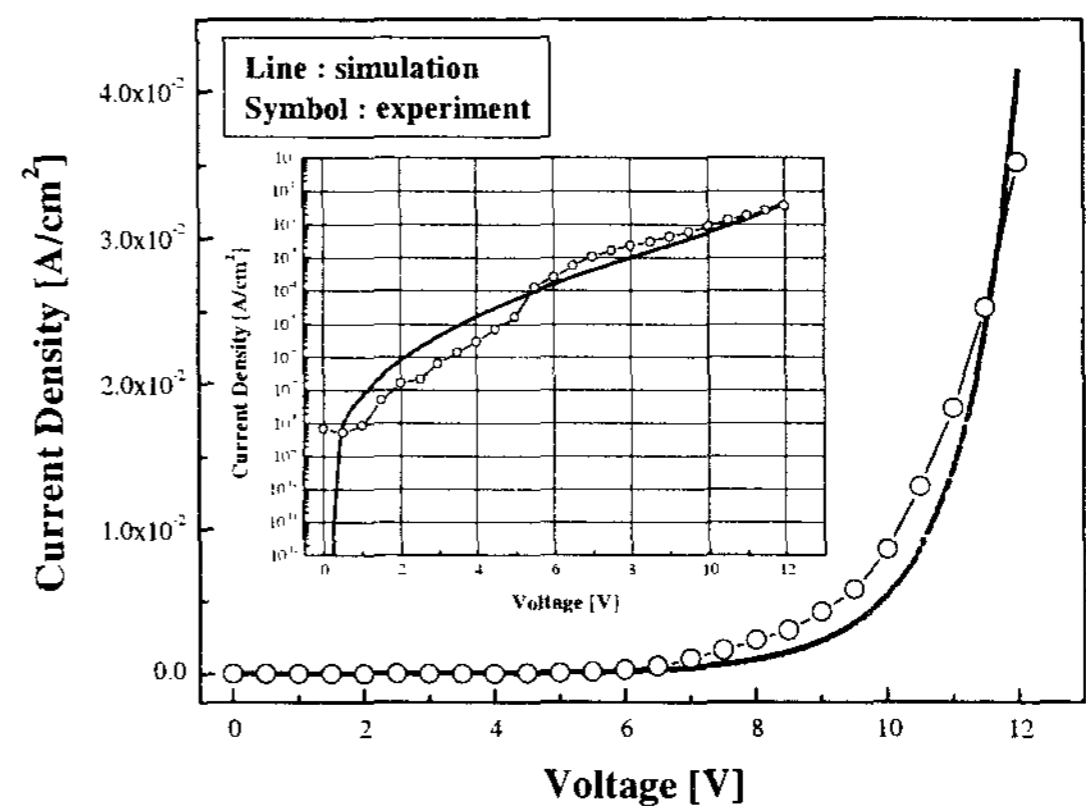


Figure 1. Simulated and measured current-voltage characteristics, inset; a semilogarithmic scale data.

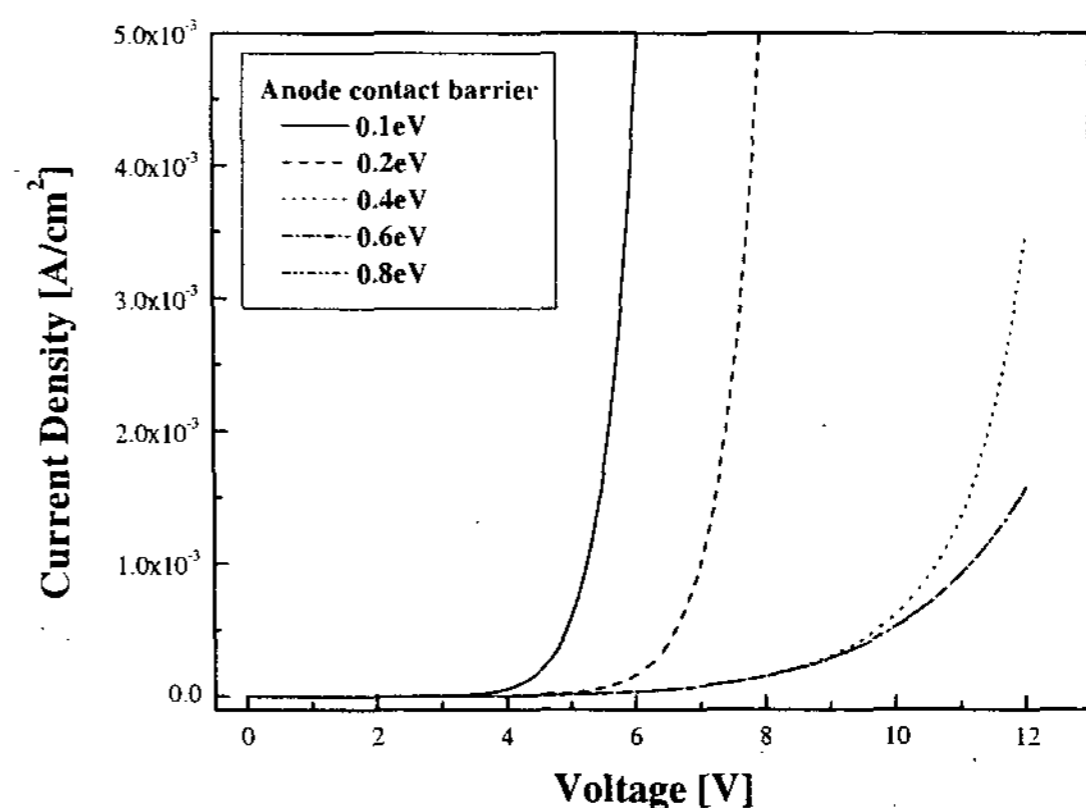


Figure 2. Simulated current-voltage characteristics with the barrier height of the anode-HTL contact.

optical and electrical characteristics of OLEDs are greatly improved, which is due to the hole injecting barrier lowering and the elevation of the anode-HTL interface properties [10]. Above 0.4eV, the turn on bias is abruptly increased compared with the case of 0.1eV and 0.2eV barrier height. For the barrier height less than about 0.3eV, the charge carrier injecting contact is space charge limited and Ohmic contact. Consequently, the carrier injecting contact plays the part of the reservoir of the charge carriers. For the larger barrier height, the current passing over the electrode-organic layer contact is the injection limited. This is comparable with the results in the other literature [11].

The spatial distributions of the hole and electron concentration for different hole injecting barrier height values are shown in figure 3, where the upper panel is the hole concentration profile, and the lower the electron concentration profile. The left of the horizontal axis represents the hole injecting contact. The holes and electrons are accumulated at the organic-organic interface, and these accumulated charge carriers contribute to the recombination at the internal interface. With the barrier height increasing, the hole concentration in the HTL side and the accumulated hole concentration at the internal interface are increased. In the lower panel, the electron concentrations are decreased with the barrier height lowering. This is due to the recombination in the ETL side close to the internal interface. For the barrier height less than 0.2eV, as the hole is easy injected into the HTL, the recombination rate increases by the balance of the hole and electron concentration (figure 4).

The recombination rate profile with hole injecting barrier height is shown in figure 4. The significant recombination rate is observed in the ETL close to the internal interface. As the lower barrier height less than 0.2eV, the narrower width of the recombination zone is observed. This is due to the balance of the hole and electron concentration, which is expected to contribute the higher recombination rate.

The recombination rates with biases are shown in figure 5. The figure 5(a) is for the barrier height of

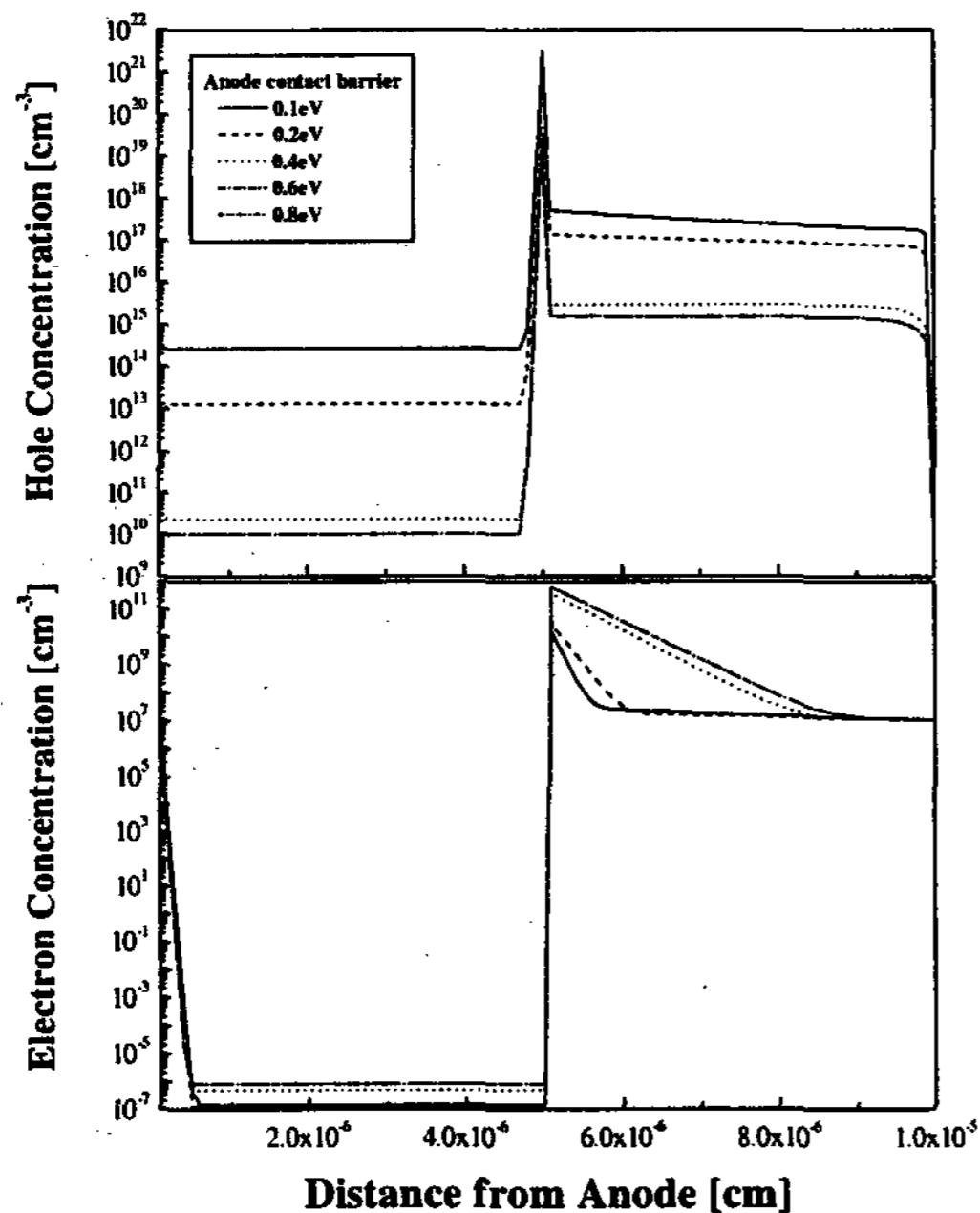


Figure 3. Spatial distribution of the charge carrier concentration, upper panel; hole concentration, lower panel; electron concentration.

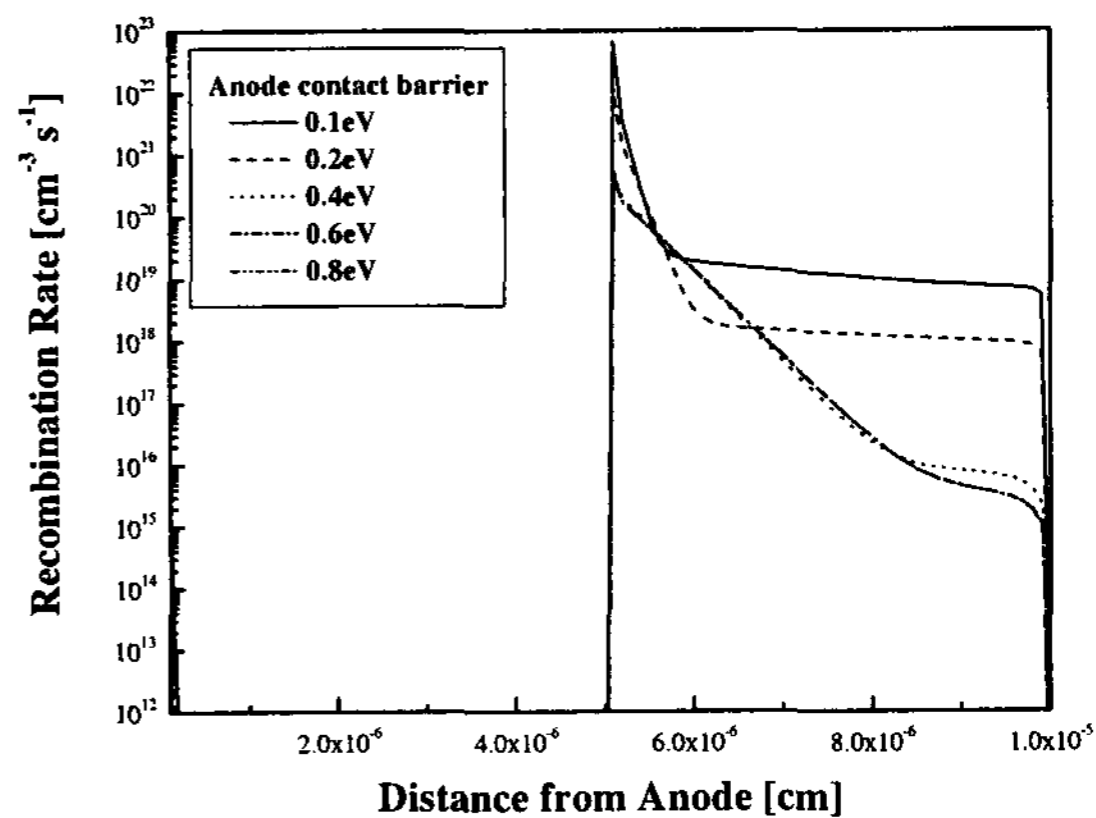
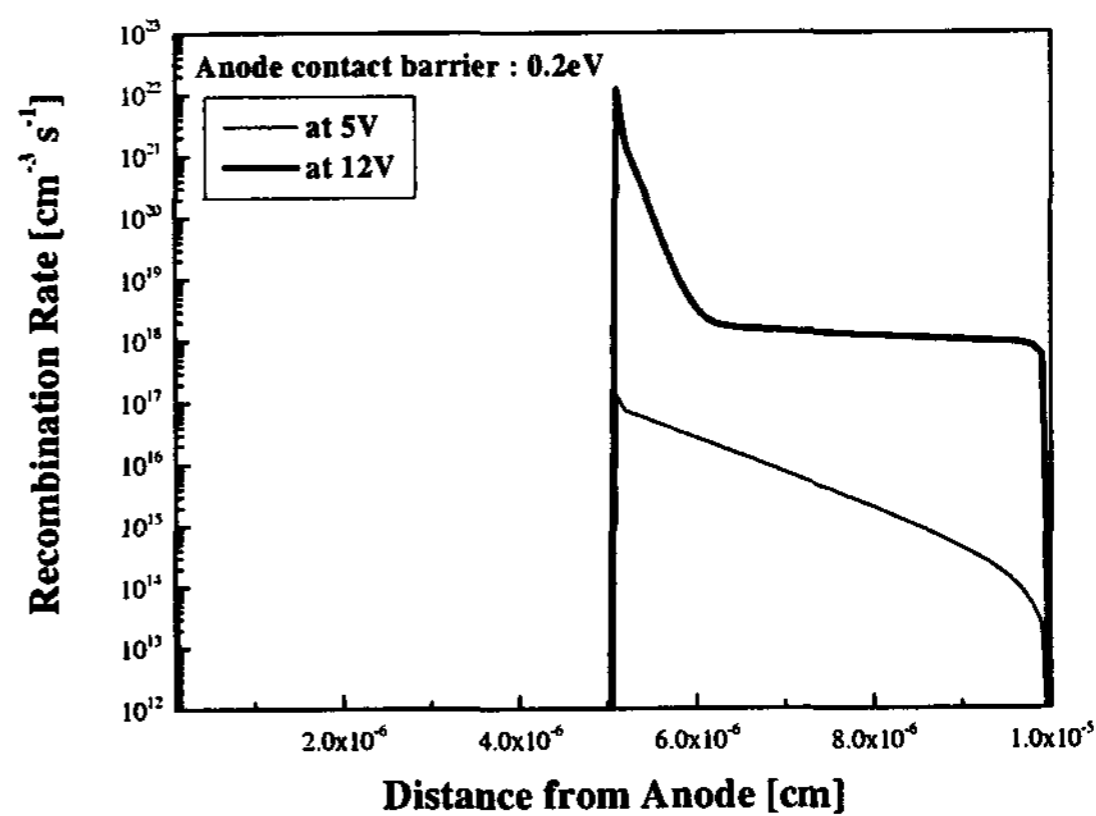
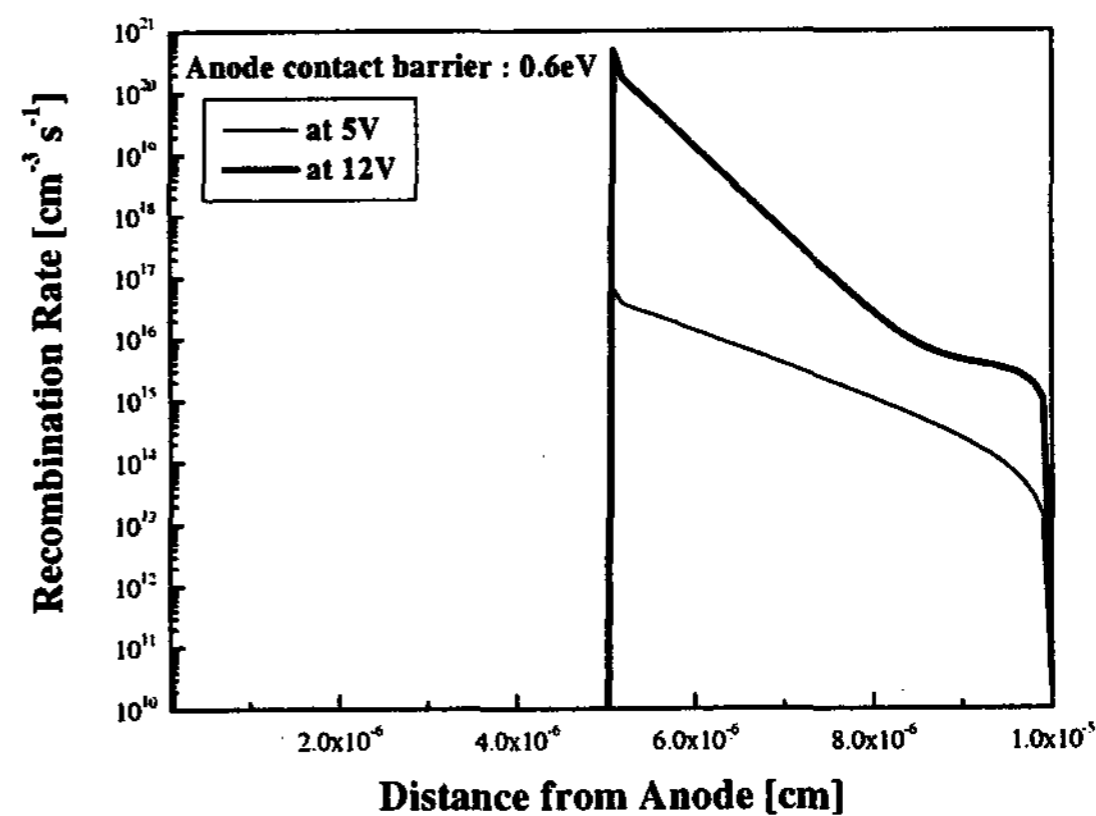


Figure 4. Spatial distribution of the recombination rate.



(a)



(b)

Figure 5. Recombination rate profiles with bias, hole injecting barrier height; (a) 0.2eV, (b) 0.6eV.

0.2eV, the figure 5(b) for the barrier height of 0.6eV. At the higher bias, the narrower recombination zones are formed in both data, and the width of the recombination zone with the lower barrier height is narrower than that with the higher barrier height. When the low bias is applied, the recombination rates are broadly distributed in the ETL side, which are nearly similar to the both data.

4. Summary

The numerical device model for the electrical characteristics of the double layer OLEDs was presented. The simulated current-voltage characteristics were very good agreement with the measured data, which indicates the device model of OLEDs in this study is realistic. With the reduction of the hole injecting contact barrier height, the more holes are injected into the HTL, which contribute to the improvement of the OLEDs characteristics. We expect that our simulation program of the OLEDs is helpful to the understanding of the various experimental results and the organic device physics. If the further research for the various parameters of the different multilayer structures is achieved, the details of the electrical properties and the electric conduction mechanisms for the OLEDs will be fully understood.

5. Acknowledgement

This work was supported by Korea Ministry of Commerce, Industry, and Energy.

6. References

- [1] P.W.M. Blom and J.M. de Jong, *IEEE J. Selected Topics in Quantum Electronincs*, 4, 105 (1998).
- [2] J. Staudigel, M. Stößel, F. Steuber, and .Simmerer, *J. Appl. Phys.*, 86, 3895, (1999).
- [3] B.K. Crone, P.S. Davids, I.H. Campbell, and D.L. Smith, *J. Appl. Phys.*, 87, 1974 (2000).
- [4] E. Tutis, M.N. Bussac, B. Masenelli, M. Carrard, and L. Zuppiroli, *J. Appl. Phys.*, 89, 430 (2001).
- [5] E. Tutis, D. Berner, and L. Zuppiroli, *J. Appl. Phys.*, 93, 4594 (2003).
- [6] Y.S. Lee, J.H. Park, and J.S. Choi, *SID 03 DIGEST*, 542 (2003).
- [7] Y.N. Gartstein and E.M. Conwell, *Chem. Phys. Lett.*, 245, 351, (1995).
- [8] A. de Mari, *Solid-State Electronics*, 11, 33, (1968).
- [9] A.D. Sutherland, *Solid-State Electronics*, 23, 1085, (1980).
- [10] J.H. Park, Y.S. Lee, Y. H. Kwak, and J.S. Choi, *IMID 01 DIGEST*, 623 (2001).
- [11] P.S. Davids, I.H. Campbell, and D.L. Smith, *J. Appl. Phys.*, 82, p. 6319, (1997).